HiSST: 3rd International Conference on
High-Speed Vehicle Science & Technology
14–19 April 2024, Busan, Korea

Design of a truncated ideal nozzle for a re-usable first stage launcher

Sebastian Karl [1], *Tamas Bykerk* [2] *and Mariasole Laureti* [3]

Abstract

This paper presents the design of a truncated ideal nozzle (TIC) for the *RFZ model*, a generic, open source geometry of a re-usable launcher in vertical take of - vertical landing (VTVL) configuration. This new nozzle is designed for methane fueled engines, to be more in line with current trends for re-usable launch systems. The design methodology is presented, along with some internal flow calculations which compare the new shape with the existing nozzle which has a parabolic thrust optimized (TOC) contour. It was found that at the same expansion ratio, the performance of the new nozzle is identical to the existing parabolic one. As expected, the TIC-design results in a slight elongation of the nozzle extension. Due to the absence of internal shocks and the resulting smooth outflow profiles the TIC configuration is considered to be more robust for the present standard test cases and outflow profiles are easier to implement in setups for CFD-rebuilding. The geometry of the new nozzle and results are made openly available to the research community to promote collaboration in understanding the design challenges associated with re-usable launchers.

Keywords: *CFD, nozzle desgin, RFZ-Model, re-usable launcher, VTVL*

1. Introduction

Aeronautical engineers have a long history of developing standardized models for wind tunnel calibrations and data comparisons between facilities. They are extremely useful in providing baseline datasets for correlation of results, data repeatability over time and verifying model installation or data acquisition systems. Reference models are also particularly relevant from the perspective of numerical analyses, where different codes can be directly compared with each other or assumptions and solver settings can be experimented with to determine solution sensitivity to certain parameters. Standardized reference models typically fulfill two main criteria. Firstly, they are simplistic in shape with a precisely defined geometry and secondly, they are representative of realistic configurations to ensure that the results are relevant. Examples of existing standard models include the AGARD-B [4], ONERA-M [6] and the Standard Dynamics Model (SDM) [2], which have been circulating for decades. Recently, models such as the NASA CRM [12] and the SSAM-Gen5 [7] provide more up to date and relevant aircraft geometries from the past 10 to 20 years.

Until recently, the space community was lacking such a model. This paper deals with the recently released, generic, open source re-usable launch vehicle (RLV), the *RFZ model*, which has been developed to serve as a consistent validation case to promote collaboration and further research into the technical challenges associated with VTVL-RLVs [3]. All relevant data are openly available on the *ZENODO* platform [1]. Currently, the data includes detailed geometries, trajectory data, estimates for the center of gravity, engine operating conditions and nozzle geometries as well as numerical reference data for the un-propelled entry flight.

This paper briefly describes the geometry of the *RFZ model* in section 2. Then, in section 3, the numerical tools used for the present analyses are introduced. The existing thrust-optimized parabolic nozzle was designed using the RAO-method[3]. Numerical results of CFD flow field simulations and resulting performance figures are discussed in section 4. Next, an overview of the design methodology

[1] *DLR - Institute of Aerodynamics and Flow Technology, Göttingen, sebastian.karl@dlr.de*
[2] *DLR - Institute of Aerodynamics and Flow Technology, Göttingen, tamas.bykerk@dlr.de*
[3] *DLR - Institute of Aerodynamics and Flow Technology, Göttingen, mariasole.laureti@dlr.de*

for an alternative nozzle with a truncated ideal contour (TIC) will be given in section 5. Finally, flow field results and performance figures of the final TIC design will be presented in section 6. While maintaining the overall performance characteristics, the resulting outflow profiles are smooth and, contrary to the parabolic nozzle, no internal shocks are present. This simplifies the treatment of the exhaust jets in numerical simulations.

2. Reference configuration

The main characteristics of the *RFZ model* are based on the SpaceX Falcon 9. The existing different geometrical setups for the launch, entry and landing phases are presented in figure 1. Falcon 9 was chosen as a baseline because it represents a functioning configuration as the only re-usable launch vehicle which is regularly used for carrying payloads into earth orbit. The geometry was generated using drawings and images of the Falcon 9 freely available on the internet. The vehicle is 70 meters long with a stage 1 diameter of 3.66 meters. Some external features of the outer mold line have been omitted in the interest of keeping the vehicle geometry as simple as possible, while still representing the required complexity and main components of a RLV. An example of this is the substitution of the grid fins with planar fins. Grid fins require a large and complex spatial resolution to be represented numerically, resulting in a substantial additional amount of computational expense. In addition, they would be difficult to manufacture on a small scale for wind tunnel models. Hinge points for the landing legs and externally run lines are also examples of items which have been neglected for simplicity. Along with the various configurations, representative trajectories, center of gravity assessments and engine state data exists for the rebuilding of different flight phases.

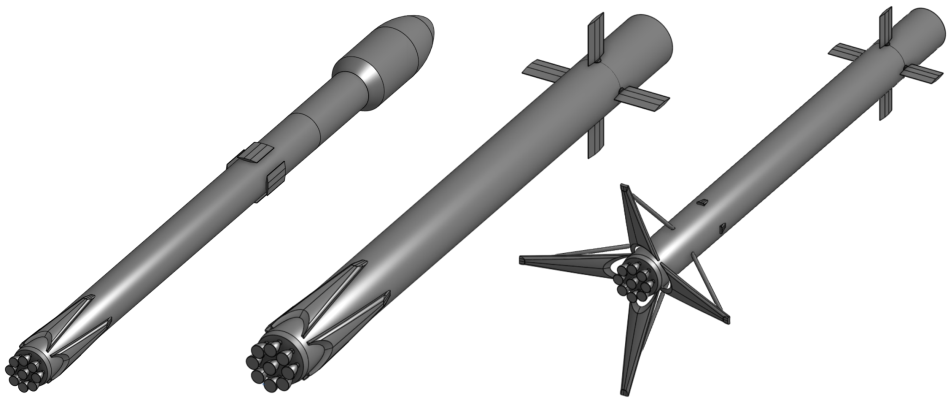

Fig 1. Launch, entry and landing configuration of the *RFZ model*

An example reference data which is already available on the ZENODO platform is shown in figure 2. It shows base heat flux and pressure distributions from numerical simulation for an un-propelled atmospheric entry at 1700 m/s and 10 deg angle of attack.

The present configuration features a cluster of 9 parabolic thrust nozzles with an expansion ratio of 16. The combustor conditions were initially chosen to be similar the Falcon-Merlin with a total pressure of 108 bar for kerosene / oxygen combustion at an oxidizer to fuel ratio of 2.35. The investigation and quantification of plume interaction effects which are typical for the operation of dense nozzle clusters are one of the main scopes of the proposed standardized reference model. This paper investigates the effect of the transition to Methane fuel and the application of ideal thrust nozzle contours to widen the range of application towards more recent trends in the development of launch systems and to further simplify the boundary conditions for numerical rebuilding.

3. Numerical model

All CFD simulations in this study were done with the DLR TAU Code [10] which is a second order finite-volume solver for the Navier-Stokes equations. The present computations are performed with

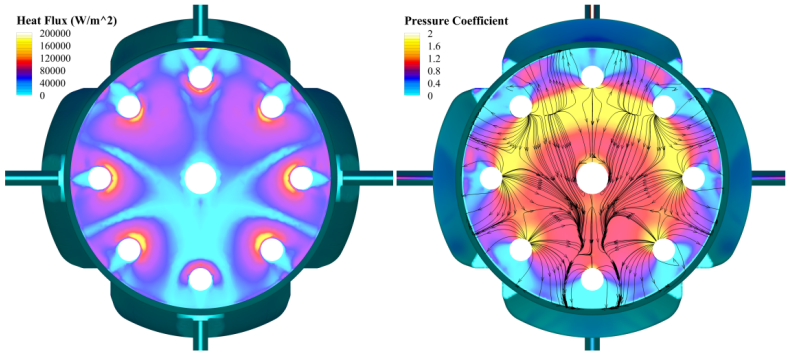

Fig 2. Example of available reference data: base heat flux and pressure distributions

an AUSMDV upwind solver for the inviscid fluxes. The non-equilibrium model is based on a finite-rate reaction rate model from Slavinskaya [13] with 23 species and 67 steps. Pre-generated lookup tables of the C-H-O-system with the same set of species as used for the non-equilibrium model were used for the equilibrium investigations. Transport coefficients (viscosity and heat conductivity) are modeled from species curve-fits and Wilke's mixture rules. Turbulence is treated with a RANS approach employing the Spalart-Allmaras one-equation eddy-viscosity model [14]. A typical computational grid with the applied boundary conditions is shown in figure 3.

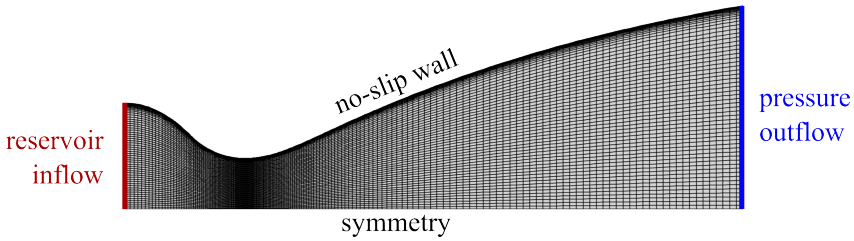

Fig 3. Computational grid and boundary conditions

The inflow is treated with a reservoir boundary conditions. Here, the total pressure and the total temperature are prescribed. Both are evaluated from the CEA equilibrium solver [8] for the given combustor pressure and oxidizer to fuel ratio. The static pressure and static density at the inflow plane are then evaluated using isentropic expansion in chemical equilibrium from the prescribed total conditions to the current inflow velocity. Hence, as required for a subsonic inflow, two state variables are prescribed (pressure and density) and one is allowed to vary (velocity). At the outflow plane, an exit pressure condition is imposed in a flux-based boundary condition. Hence, an outer state is prescribed which is a copy of the inner state in which the static pressure is replaced by the prescribed exit value. Then, an upwind-solver is used to determine the boundary flux. This approach has the advantage that the transition from subsonic to supersonic outflow is treated in a numerically consistent way. At the no-slip wall condition, a constant temperature of 500 K was imposed. The mesh resolution at the viscous wall was chosen such that the laminar sublayer is sufficiently resolved (y^+ around 1) as required for the low-Re formulation of the employed turbulence model.

The method of characteristics was used to design the initial contour of the nozzle extension. The idea of the method is to decouple the irrotational, inviscid, steady Euler equation for supersonic flow to a set of ordinary differential equations which can be solved analytically along characteristic directions. The resulting Riemann invariants are a constant sum of the Prandtl-Meyer-Angle and the local flow angle along the Mach lines in the flow field. The present computations were performed with *IMOC*[9] which represents a basic implementation for a constant ratio of specific heats in flow fields without discontinuities.

4. Performance and properties of the existing parabolic nozzle

The first stage engines of the standard *RFZ model* are largely based on the Merlin 1D+ from the SpaceX Falcon 9 launcher. The nozzle has an expansion ratio of 16:1 with a throat area of 0.042 m^2 as shown in Figure 4. The low expansion ratio is needed due to the tight clustering of the nozzles. Further, it reduces flow separation inside the nozzle extension during throttled operation at sea level in the course of landing. A nozzle contour was generated using the method outlined by Rao in the openly available code *Ravi4Ram*[11] with a length ratio of 80%. The initial operating conditions of the nozzle are evaluated from the assumption that kerosine is burned at a combustion chamber pressure of 108 bar and an oxidizer-to-fuel ratio of 2.35. Results from CFD analysis of this nozzle with the kerosene operating conditions are shown in figure 5. The Mach number contours in part (a) of this figure show the formation of a strong internal shock due to the curvature jump at the intersection of the throat area and the nozzle extension. This shock is further highlighted by contours of negative velocity divergence (as an indicator for local compression). The effect of the chemistry model (equilibrum vs non-equilibrium) is negligible for the flow structure (part (a)) and the flow properties at the nozzle exit (part (c)). Nevertheless, differences can be observed in the axial mass fraction distribution in part (b) of figure 5. The flow tends to freeze in the last third of the nozzle extension and the species composition in non-equilibrium does not follow the rapid changes of pressure and temperature due to the impact of the internal shock. However, the differences remain small and the effect of chemical non-equilibrium on the bulk flow properties is negligible.

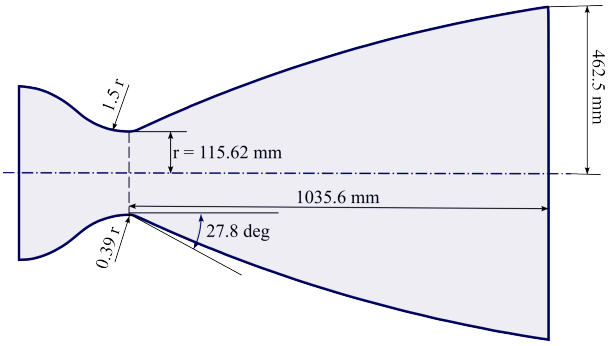

Fig 4. Stage 1 nozzle contour

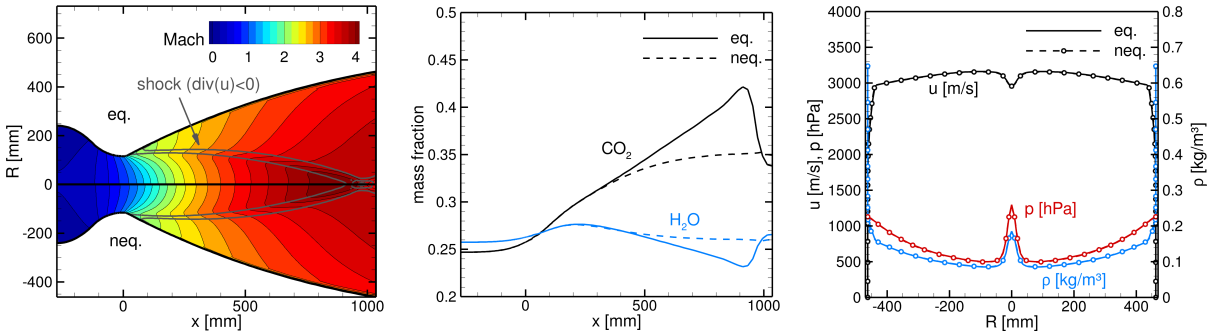

(a) flow structure **(b)** axial species distribution **(c)** exit profiles

Fig 5. CFD results for the parabolic nozzle with kerosene fuel

To predict the nozzle performance for methane fuel, a preliminary analysis with CEA [8] was performed assuming an oxidizer to fuel ratio of 3.5. It was found that a slight reduction of combustor pressure to 106 bar yields the same thrust as for the kerosene case. The results of the subsequent CFD simulation of the nozzle flow are shown in figure 6. The general characteristics are very similar. The effect of chemical non-equilibrium is slightly enhanced and the static pressure at the center of the nozzle exit

varies by about 5% between the equilibrium and the non-equilibrium cases. However, this is limited only to a small zone around the reflection point of the internal shock.

The non-equilibrium effects on the general performance characteristics are very limited. A summary of the relevant figures is given in table 1. The, compared to its theoretical maximum, low vacuum specific impulse, I_{sp}, is mainly due to small expansion ratio of the nozzle. As intended, the total thrust differs by less then 1% between the kerosene and methane fueled cases.

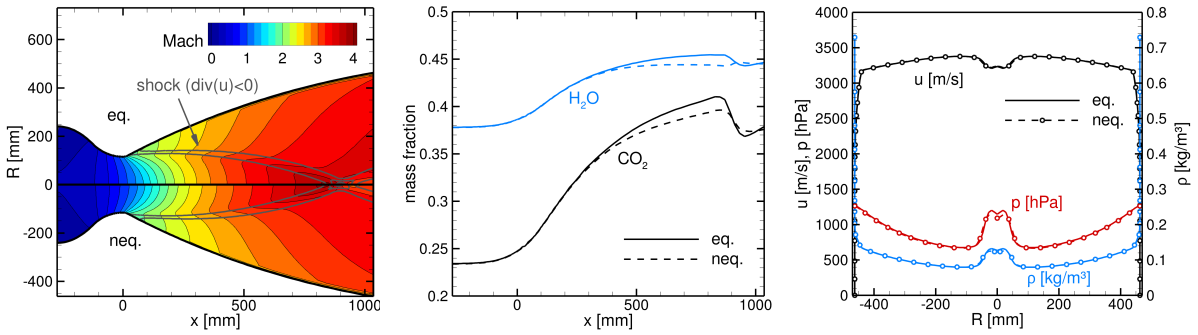

(a) flow structure **(b)** axial species distribution **(c)** exit profiles

Fig 6. CFD results for the parabolic nozzle with methane fuel

Table 1. Performance of the parabolic Rao-nozzle for different fuels

	Kerosene (108 bar)		**Methane (106 bar)**	
	equilibrium	nonequilibrium	equilibrium	nonequilibrium
vacuum thrust	803.1 kN	803.5 kN	809.0 kN	808.9 kN
mass flux	250.7 kg/s	250.5 kg/s	231.9 kg/s	231.8 kg/s
vacuum I_{sp}	3203 m/s	3208 m/s	3489 m/s	3490 m/s

5. Design of the truncated-ideal-contour nozzle (TIC)

For the design of the ideal nozzle contour, a conical template flow field was generated by CFD simulation with the chemical equilibrium model using the throat radius and maximum opening angle of the existing prabolic nozzle. The throat contour was modified to avoid jumps in the curvature. This was done by prescribing a continuous distribution of curvature and subsequent double integration to obtain the radius distribution. The main design constraints for the nozzle are the same expansion ratio, the same throat area and the same thrust as for the parabolic nozzle. In a first step, three different initial characteristics (right running Mach lines) were extracted from the conical template flow which correspond to a maximum Mach number at the central axis of 3.4, 3.5 and 3.7. They serve as start characteristics for the design of 3 different ideal nozzles for the exit Mach numbers which are identical to the maximum Mach of the start characteristic (i.e. 3.4, 3.5 and 3.7). This also results in 3 different total area ratios. The conical template flow and the extracted start characteristics are shown in figure 7.

In the next step, the start characteristics are used together with their associated design characteristics to obtain streamlines for the walls of the ideal nozzles for the different Mach numbers as illustrated in figure 8. The design characteristic is simply a left running Mach line with a constant Mach number and flow angle imposed as boundary conditions at the nozzle exit. The Mach number is identical to the value of the start characteristic at the intersection point at the central symmetry line as both characteristics share this point. Both boundary characteristics (start from conical template flow and design as boundary condition for the ideal nozzle) fully specify the flow in the nozzle extension. An example of the characteristic mesh is shown in figure 8. The sum of the Prandtl-Meyer angle and the local flow angle is constant on the right running lines emanating from the design characteristic and the left running lines emanating from the

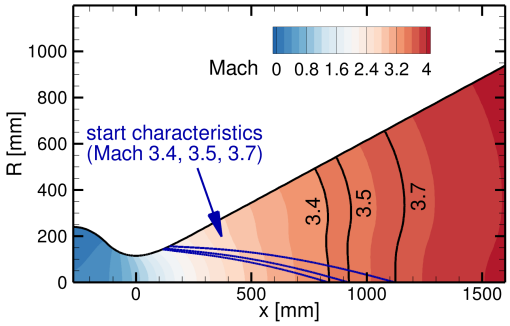

Fig 7. CFD result for the initial conical nozzle with start characteristics

start characteristic. Hence, these two unknowns can be solved for every point in the flow successively. The procedure starts at the intersection between the two boundary lines at the axis. The geometry of the mesh is then a determined by the Mach lines being computed form the local Mach number (as a function of the Prandtl-Meyer angle) and the local flow angle. After the mesh of characteristics is established, the nozzle contour is simply obtained by streamline tracing as shown in the figure. The main approximations in the applied method are the assumptions of a constant ratio of specific heats ($\gamma = 1.1$) and of inviscid flow (no boundary layer).

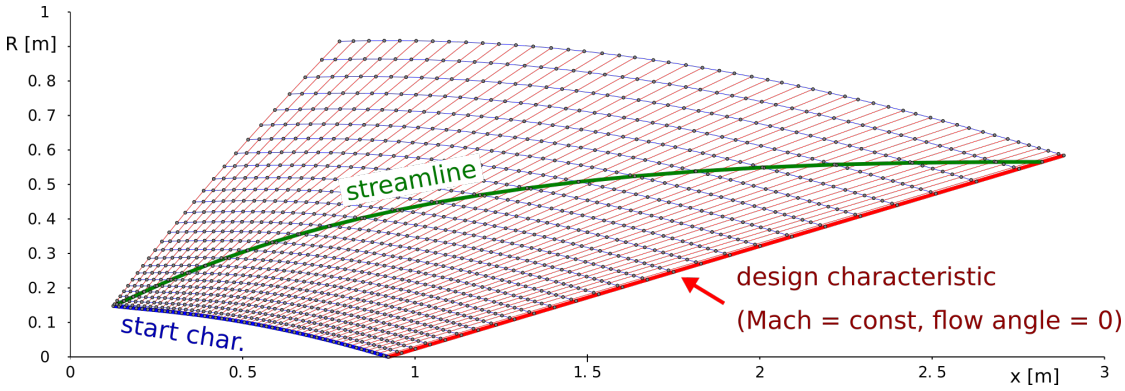

Fig 8. Mesh of characteristics and streamline traced nozzle contour

The nozzle contours which result from the different design Mach numbers are shown in figure 9. The limiting radius for the area ratio of 16 is also indicated in this figure. A truncation of the ideal contours at the given area ratio would result in the shortest nozzle for the highest design Mach number. This is due to the larger resulting initial opening angle at large Mach numbers. The corresponding truncation lengths are indicated by the green arrows.

The performance of the ideal nozzles for different area ratios is shown in figure 10. The results are obtained by inviscid CFD analysis of the initial MOC-designs. Because the boundary layer is neglected, it is likely that the thrust is slightly overestimated. The black curves indicate the inviscid thrust for different design Mach numbers and the red curves show the corresponding length of the nozzle after truncation to the given area ratio. The length and thrust of the parabolic baseline nozzle is depicted by the dots. As a general trend, a smaller design Mach number results in higher thrust and a longer nozzle for a fixed given area ratio. The performance and size of all nozzles is in the same ballpark as for the parabolic baseline design obtained from the Rao-method.

The design Mach number of 3.5 was chosen for the final design optimization. It represents an optimum compromise between performance and nozzle length. For the optimizing procedure, the nozzle was truncated to a length of 1.5 m (the original length of the complete ideal nozzle extension was 2.8 m).

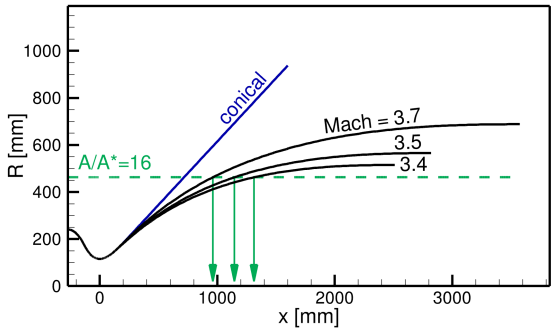

Fig 9. Resulting contours for different design Mach numbers

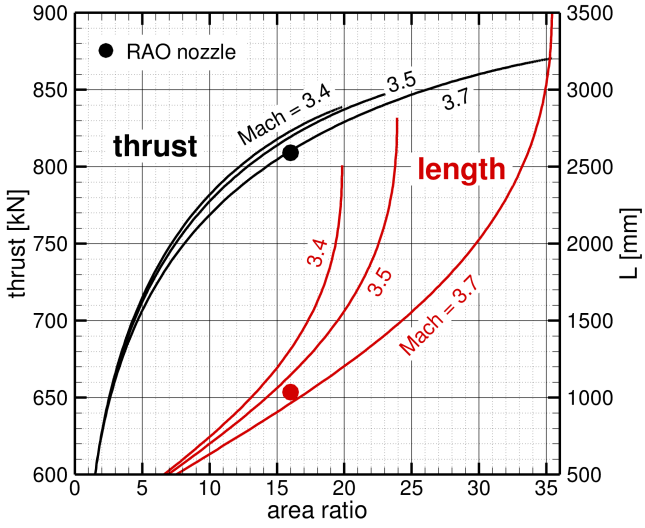

Fig 10. Performance map for different design Mach numbers

The length of 1.5 m guarantees that the desired area ratio of 16 is reached even for modified contours. The result of a viscous CFD computation of the initial MOC-contour in thermo-chemical equilibrium shown in figure 11.

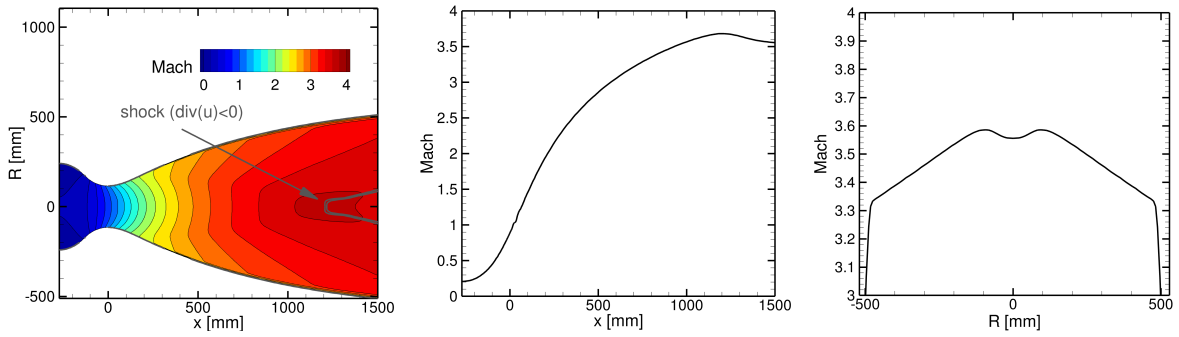

(a) flow structure **(b)** axial Mach number **(c)** exit Mach number

Fig 11. Mach number distribution of the initial nozzle contour

It is visible from the results in figure 11 that neglecting of the boundary layer and the assumption of

a constant ratio of specific heats in the MOC design results in a non-perfect nozzle contour. The Mach number on the symmetry axis is not constant at the downstream end and in the central part of the exit plane. Hence, an optimization of the contour based on CFD with equilibrium thermo-chemistry and viscous turbulent boundary layers was performed. This optimization is based on the parametrization of the nozzle contour using its second derivative (curvature). The physical contour is obtained by double integration of the spline-interpolated curvature. This ensures a steady curvature and results in a contour which will not produce internal shocks. The target function of the optimization is an ideal Mach number distribution (constant downstream of the intersection of the start characteristic on the axis and on the central part of the outflow plane). If the Mach number deviates from its ideal behavior, the contour is adapted accordingly. This process is schematically illustrated in figure 12. The underlying idea is to use right running Mach lines (characteristics) to identify the surface region which is responsible for a deviation in the Mach number field. If the local Mach number is too low, the curvature at the corresponding surface location is decreased, if the Mach number is too large, the curvature is increased. The hyperbolic behavior of the supersonic flow field suggests that the adaptations are applied successively in downstream direction. This means that first the Mach number on the symmetry axis is optimized from the end of the start characteristic to the nozzle end and then the exit profile is adapted from the center in outward direction.

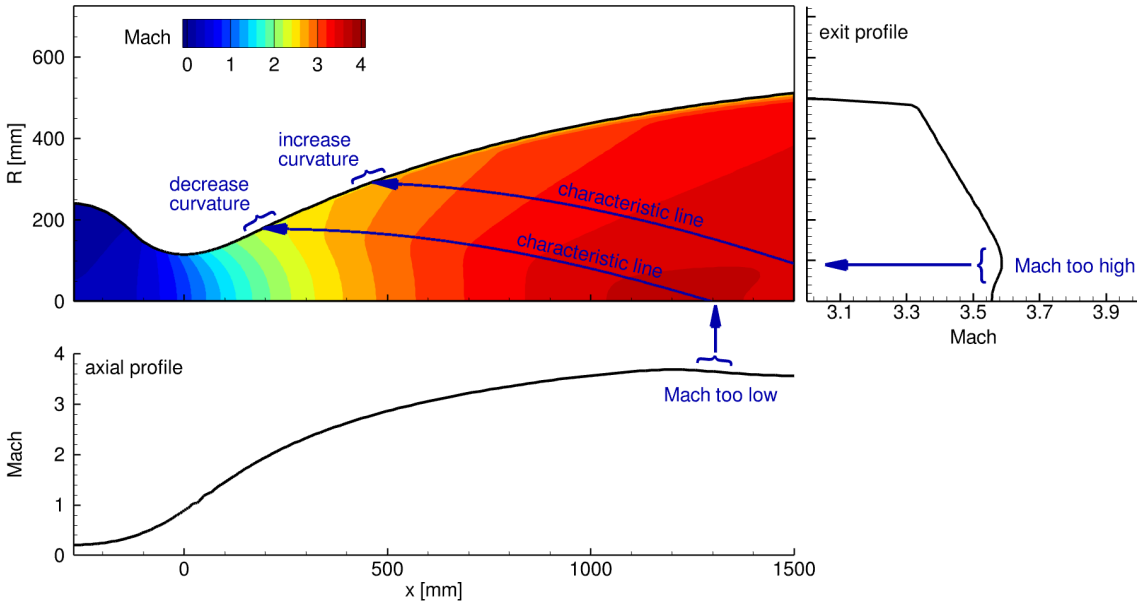

Fig 12. Schematics of the optimization procedure

Figure 13 shows the curvature and radius distributions of the initial and final nozzle contour. The parametrization points are indicated by circles and the curves were obtained by spline interpolation from those points (curvature) and double integration of the curvature (radius). The green curve in the right part of the figure shows the absolute difference between the radii of the initial and optimized contours. It can be seen that the modifications in the radius remain below a low value of 3 mm.

The resulting Mach number distribution of the optimized nozzle contour is shown in figure 14. The improvement is clearly visible by comparison with the initial profile in figure 11. The Mach variations in the regions where a constant Mach number is expected to be produced by the ideal nozzle extension stay below 0.1%.

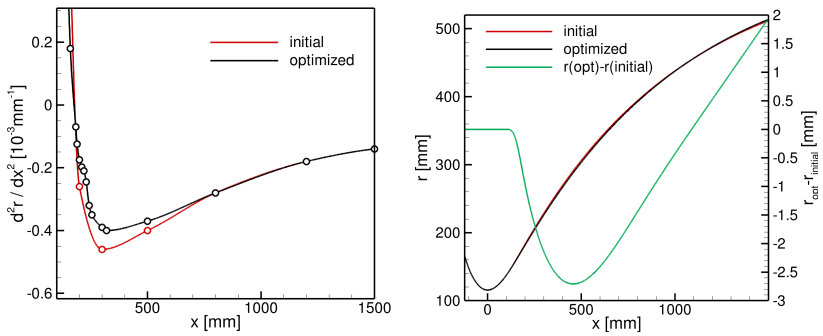

(a) curvature **(b)** contour

Fig 13. Parametrization of curvature and resulting nozzle contours before and after the optimization

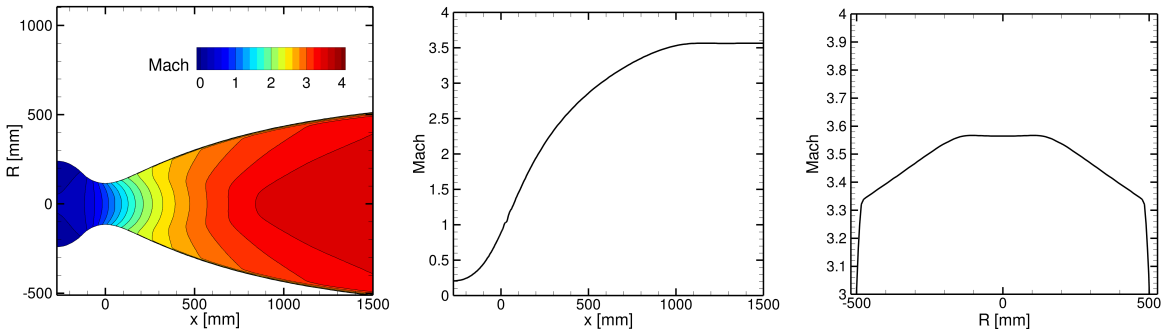

(a) flow structure **(b)** axial Mach number **(c)** exit Mach number

Fig 14. Mach number distribution of the optimized nozzle contour

6. Performance and flow field properties of the final TIC nozzle

In the last step, the nozzle was truncated to an area ratio of 16. This results in a length of the nozzle extension (measured from the throat) of 1135 mm which is only slightly longer than the original parabolic configuration (1036 mm). The flow properties (Mach number field, species distribution on the symmetry axis and exit flow profiles) are shown in figure 15 for the cases of chemical equilibrium and non-equilibrium. Again, the impact of chemical non-equilibrium is negligible and even less as for the parabolic nozzle. This is due to the absence of internal shocks and the resulting reduced gradients of the bulk flow properties in the flow field.

In figure 16, the flow field and nozzle exit profiles are compared to the parabolic nozzle. The new nozzle does not have internal shocks which results in a smoother variation of flow properties at the nozzle exit. The distributions of flow velocity (the total velocity is shown), Mach number, pressure and flow angle at the nozzle exit are very similar for the parabolic and TIC designs. Note that the static wall pressure at the nozzle exit is almost identical between the TIC and parabolic nozzles, hence the onset of flow separation at throttled sea-level conditions is likely to happen at the same nozzle pressure ratio. Hence, there is no loss of operational robustness when applying the TIC nozzle.

Global properties and performance figures are given in table 2. The thrust, specific impulse, divergence angle at the exit and static wall pressure at the exit are almost identical between the TIC and the parabolic baseline. This also represents a verification of the correct design of the existing parabolic nozzle. The TIC nozzle is, as expected, slightly longer (by about 10%). The surface area of the nozzle extension of the TIC design is about 6% larger, hence, it is likely that the ideal nozzle will be slightly heavier.

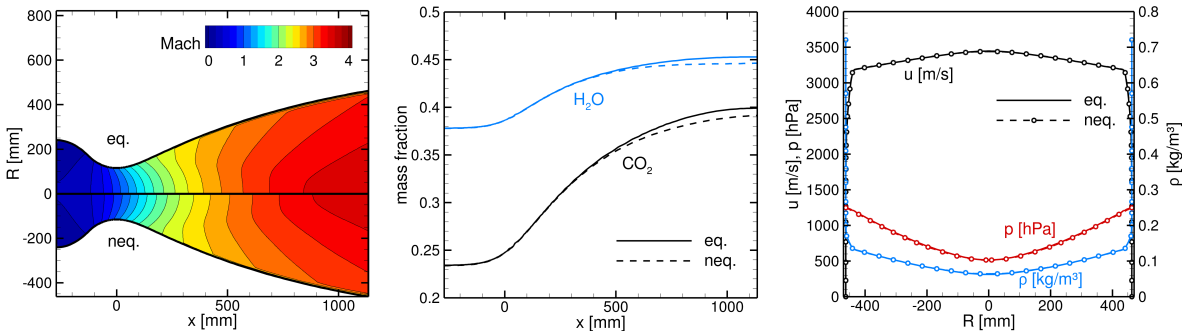

(a) flow structure **(b)** axial species distribution **(c)** exit profiles

Fig 15. CFD results for the truncated ideal nozzle with methane fuel

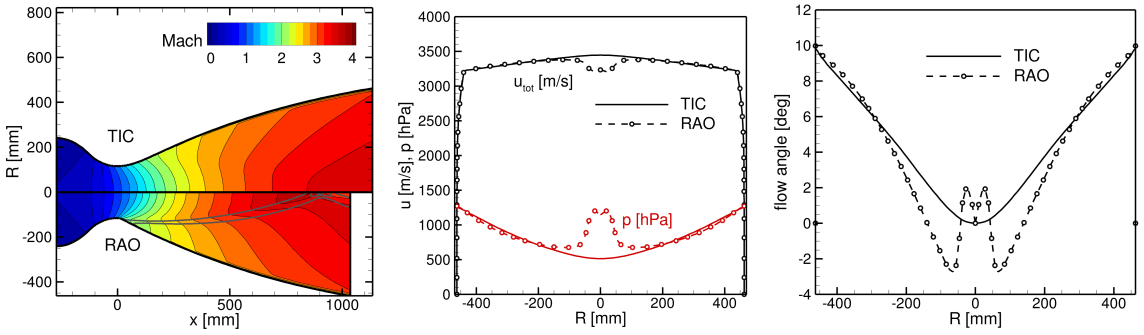

(a) flow structure **(b)** exit velocity and pressure **(c)** exit flow angle

Fig 16. Comparison of the TIC and RAO nozzles

Table 2. Comparison of TIC and RAO performance figures

	TIC		**Parabolic (RAO)**	
	equilibrium	nonequilibrium	equilibrium	nonequilibrium
vacuum thrust	808.3 kN	808.3 kN	809.0 kN	808.9 kN
mass flux	231.9 kg/s	231.8 kg/s	231.9 kg/s	231.8 kg/s
vacuum I_{sp}	3485 m/s	3487 m/s	3489 m/s	3490 m/s
Length from throat	1135 mm		1036 mm	
Surface from throat	2.30 m²		2.17 m²	
Contour angle at exit	9.75 deg		9.89 deg	
Max. contour angle	24.7 deg		27.7 deg	
Wall pressure at exit	125.8 kPa	124.9 kPa	127.4 kPa	126.4 kPa

7. Summary

A truncated ideal contour (TIC) nozzle was designed for the *RFZ model* which is a generic open source configuration of a re-usable VTVL launcher. This nozzle has an identical area ratio and very similar performance parameters as the previously designed parabolic nozzle. This also serves as a cross-validation of both designs.

The advantages of the new TIC-nozzle are:

- Smooth outflow profiles which are easier to implement for CFD rebuilding of the test case (i.e. by Dirichlet conditions at the nozzle exit),
- Smooth flow field without internal shocks inhibits the occurrence of restricted shock separation [5]. Hence, the TIC design enables improved startup and shutdown properties with reduced side loads.

And its main disadvantage is:

- Slightly longer nozzle and associated larger mass of the nozzle structure.

The contours and numerical results for both configurations are available on ZENODO [1]. This enables additional studies of the influence of internal patterns or different outflow profiles on the wake flow and plume-plume-interaction phenomena of the rocket configuration.

References

[1] The rfz model - a standard model for the investigation of aerodynamic and aerothermal loads on a re-usable launch vehicle. `https://zenodo.org/communities/rfz-model`. Accessed: 2024-01-16.

[2] M. Beyers and X. Huang. Subsonic Aerodynamic Coefficients of the SDM at Angles of Attack up to 90°. Technical report, NRC, Ottowa, Canada, 1990.

[3] Tamas Bykerk. A standard model for the investigation of aerodynamic and aerothermal loads on a re-usable launch vehicle. In *Aerospace Europe Conference 2023 - 10th EUCASS - 9th CEAS, Lausanne, Switzerland*, 2023.

[4] North Atlantic Treaty Organization. Advisory Group for Aeronautical Research and Development. Wind tunnel calibration models - agard specification 2. Technical report, NATO, 1958.

[5] Manuel Frey and Gerald Hagemann. Restricted shock separation in rocket nozzles. *Journal of Propulsion and Power*, 16(3):478–484, 2000.

[6] R.D. Galway and M. Mokry. Wind tunnel tests of onera aircraft models. Technical report, National Aeronautical Establishment, 1977.

[7] Nicholas F. Giannelis, Tamas Bykerk, and Gareth A. Vio. A generic model for benchmark aerodynamic analysis of fifth-generation high-performance aircraft. *Aerospace*, 10(9), 2023.

[8] S. Gordon and B. J. McBride. Computer Program for Calculation of Complex Chemical Equilibrium Compositions and Applications. Technical Report NASA Reference Publication 1311, NASA, 1996.

[9] P. Jacobs and C. M. Gourlay. An interactive method-of-characteristics program for gas-dynamic calculations. *The International Journal of Applied Engineering Education*, 7(3):242–250, 1991.

[10] Norbert Kroll, Stefan Langer, and Axel Schwöppe. The dlr flow solver tau - status and recent algorithmic developments. 01 2014.

[11] Ravi4Ram. Bell nozzle, 2023. `https://github.com/ravi4ram/Bell-Nozzle`.

[12] M. B. Rivers, J. Quest, and R. Rudnik. Comparison of the nasa common research model european transonic wind tunnel test data to nasa test data (invited). In *AIAA SciTech Forum*, Kissimmee, Florida, Jan 2015.

[13] N.A. Slavinskaya, O.J. Haidn, and J. Steelant. Kinetic modeling for high pressure, fuel - rich methane / oxygen combustion. Number AIAA 2007-0775 in 45th AIAA Aerospace Sciences Meeting and Exhibit. AIAA, 2007.

[14] P. R. Spalart and S. R. Allmaras. A one-equation turbulence model for aerodynamic flows. *Recherche Aerospatiale*, 1:5–21, 1994.